4th Conference on Biomedical Applications of Electrical Impedance Tomography

Department of Mathematics, University of Manchester Institute of Science and Technology (UMIST), April 23-25, 2003.

This meetings continues a series of meetings, dating back to the meeting in 1986 in Sheffield prior to the organisation of a European Concerted Action on EIT, the concerted action CAEIT meetings around Europe, then followed by the EPSRC network funded meetings on Biomedical Applications of EIT in London in 1998, 1999, which continued 2001, establishing the tradition of the 'London Meeting' after the Network funding had finished. In 2002 it was generally agreed among the UK EIT community to not hold a London meeting but instead to go to the 1st Mummy Range meeting on EIT at Pingree Park in Colorado. So in a way this is the 3rd 'London Meeting', except that this year it is held in Manchester! Those used to EIT meetings will recognise many familiar features, a healthy mixture of medical applications, hardware reconstruction algorithms together with some interdisciplinary papers where we have common course with geophysical and process monitoring applications. We also have the usual mixture of old-hands and newcomers to the field. You will also notice that like other meetings in the series this is a low budget operation, even more so given that this meeting has no research grant to support it. On the other hand this is the first meeting where there are trade stands which contribute a little to the funding of this meeting, and for which we are very grateful.

While unlike Pingree Park, we can not offer snow topped mountains and Moose wandering through campus, we hope you will enjoy the excursion to Castleton. We resisted the suggestion that the conference outing should be a trip to Brian Brown's birthplace and a black-pudding tasting in Bury.

This conference continues to show exciting developments in clinical applications, hardware and reconstruction in EIT, as well as increasing interest on Magnetic Induction Tomography and Magnetic Resonance EIT. We hope you enjoy the meeting.

Bill Lionheart and Richard Bayford

Programme

Wednesday 23rd April

9:30-10:30 Registration and coffee outside C19 and C24

10:30-11:15 Session 1

11:15-13:00 Session 2

13:00-14:00 Lunch in C22

14:00-15:00 Session 3

15:00-15:30 Coffee C22

15:30-17:15 Session 4

Thursday 24rd April

9:00-10:15 Session 5 Chair: Tony Peyton

10:15-10:45 Coffee C22

10:45-12:15 Session 6a Chair Huw Griffiths

12:30 Coach Leaves for Castleton, returns 18:30

10:45-12:15 Session 6b Chair Bill Lionheart

Black-box Algebraic Multigrid for the 3D Forward Problem arising in Electrical Resistance Tomography	Manuchehr Soleimani, Catherine Elizabeth Powell	42
An idea about utilizing bulk volume fraction information in local volume fraction estimation	Lasse M. Heikkinen, Robert M. West and Marko Vauhkonen	43
Use of Reconstruction Bases in Electrical Impedance Tomography	Hamid Dehghani, Nirmal Soni, and Keith D Paulsen	44
A Two-phase Electrical Impedance Tomography Algorithm using the Extended Kalman Filter	R.G Lima, F.C. Trigo, M.B.P. Amato	45
Recent Developments in Reconstruction Algorithms in EIT	W.R.B. Lionheart	46
Markov chain Monte Carlo techniques and spatial-temporal modelling for medical EIT	Sha Meng	47

12:30 Coach Leaves for Castleton, returns 18:30

Friday 25th April

9:00-11:00 Session 7 Chair: Andy Adler

Title	Authors	Page
Introduction to MR-EIT and Review of Reconstruction Algorithms	Y. Ziya İder B. Murat Eyüboğlu	50
Reconstruction of Current Density and Conductivity Distributions using One Component of Magnetic Flux Density	Ohin Kwon, Jin Keun Seo, Byung Il Lee and Eung Je Woo	48
Combined Use of MRCDI and MR-EIT for Lead Field Imaging	B. Murat Eyübŏglu and Orçun Özbek	51
Equipotential Projection Based Magnetic Resonance - Electrical Impedance Tomography (MR-EIT) and Experimental Realisation	B. Murat Eyübŏglu and Mahir S. Özdemir	53
Magnetic Resonance - Electrical Impedance Tomography (MR-EIT) using Magnetic Flux Density in One Direction and Experimental Realisation	Özlem Birgül, B. Murat Eyübŏglu and Y. Ziya İder	52
Method of Characteristics for Reconstruction in MR-EIT formulated as a system of First Order Hyperbolic Partial Differential Equations	William R.B. Lionheart, Y. Ziya İder, Serkan Onart	54

11:00-11:30 Coffee C22

11:30-12:15 Session 8 Chair: Murat Eyübŏglu

Title	Authors	Page
Three-Dimensional Forward Solver for Magnetic Resonance Electrical Impedance Tomography (MREIT) using Recessed Electrode	Eung Je Woo, Byung Il Lee, Suk Hoon Oh, Soo Yeol Lee, Min Hyeung Cho, Ohin Kwon and Jin Keun Seo	49
Finite Difference and Gradient Based solutions for MR-EIT formulated as a system of First Order Hyperbolic Partial Differential Equations	Y. Ziya İder William R.B. Lionheart Serkan Onart	55
A new Iterative Reconstruction Algorithm for MR-EIT using the Laplacian of one component of Magnetic Field Intensity	Serkan Onart, Y. Ziya İder	56

12:15-13:00 Session 9 Hamid Dehghani

Title	Authors	Page
Accounting for missing electrode data in electrical impedance tomography	Andy Adler	30
Evaluating electrode position change in an EIT System Using a 3D Finite Difference Model of the Thorax and Direct Human Measurements	Robert P. Patterson and Jie Zhang	29
3D sensitivity distributions with different electrode placement	Mengxing Tang, Wei Wang, Malcolm McCormick, Li Wang, Xiuzhen Dong	31

13:00-14:00 Lunch C22

14:00-15:15 Session 10 and close Chair: Ros Sadleir

Using Geophysical Concepts to Measure Internal Organ Resistivities

Robert P. Patterson and Andres Belalcazar

University of Minnesota USA

The field of geophysics has a 30 year history of making earth impedance measurements to map the underground. Geologists have developed theoretical techniques using various types of surface electrode arrays. Companies have produced both hardware and software systems that yield 2D and 3D images of the earth solving the inverse problem. These techniques are applied in this study to measure resisitivities of internal organs of the thorax.

Methods: A simple linear array of 10 electrodes, (10 cm long), was used to make a series of transfer impedance measurements on a human subject's back. Commercial geophysical software was used to determine lung resistivity from the measurements. In a second part of the study, a rectangular four-layer 3D finite difference model (FDM) with 820,000 control volumes was used to evaluate the accuracy of the technique. The layers of the model were: skin (0.25 cm), fat (2 cm), muscle (2 cm), and lung (12 cm) as would approximately occur when measuring from a patient's back. The resistivities for these tissues were set to 600, 2000, 400, and 1400 Ωcm, respectively. A change of the lung to 1700 Ωcm was introduced later to assess detection of physiological changes.

Results: For the human subject, the measured lung resistivity was 1600 Ωcm, which increased approximately 200 Ωcm with inspiration. In the second part, for the 4 layer FDM model, the measured resistivities in the lung (9 cm deep from skin surface) were 1362 and 1733 Ωcm.

Conclusions: The measurements observed in the humans and the model agree with published figures, and suggest that the proposed technique is feasible and offers potential for clinical applications.

Static Impedance Tomography for Diagnosing Respiratory Impairments of the Newborn.

V. Cherepenin†, V. Bardin‡, A. Karpov§, A. Korjenevsky†

†Institute of Radio-Engineering and Electronics of Russian Academy of Sciences, Russia
‡Yaroslavl State Medical Academy, Russia
§Clinical Hospital # 9, Yaroslavl, Russia

There are no methods which can be simultaneously distinguished by a diagnostic efficiency and safety for the newborns among contemporary methods for diagnosing respiratory impairments of the newborn. Static electrical impedance tomography (EITs) can meet the requirements. We measured electrical impedance of the chest of newborns with respiratory impairments of a different genesis: disease of hyaline membranes, atelectasis, meconium aspiration, congenital pneumonia. We used 16-electrode single-frequency (8 kH, 0.5 mA) single- channel electrical impedance tomograph for obtaining static imaging which had been developed in the Institute of Radio-Engineering and Electronics, Russian Academy of Science. Computerized scanning of thoracic organs of newborn was made at intercostal level 4. For the measurements we used steel round electrodes (6 mm in diameter) which were fixed around the thoracic organs of newborn by way of a rubber belt at intercostal level 4. Measurements were made when the newborn respired himself and under artificial pulmonary ventilation. We have already indicated above that:

1. healthy newborn EITs shows the lungs as zones with a comparatively high electric conductivity which is lower than in medi- astinum but higher than in spine,

2. normal anatomical correlation of EI- images of lungs and heart is visualized,

3. EI-images of airflow pathways and a respiratory zone are clearly determined.

When there is a disease of hyaline membranes EITs shows a marked double-sided increase of electric conductivity in the airflow pathways and respiratory zone. During atelectasis and congenital pneumonia a respiratory zone conductivity on the affected side and anatomic correlation of lungs and mediastinum change. Under artificial pulmonary ventilation EITs records a rhythmic change of electrical conductivity in the airflow pathways and respiratory zone: conductivity goes down while inhaling and it rises while breathing out. Further development of the EITs method (hard - and software) will enable to have a safe and informative tool to diagnose respiratory impairments of the newborns.

Changes in forced vital capacity followed by EIT in methacholine challenge test

Roberto E. Serrano †, Bruno de Lema ‡, Teresa Feixas ‡, Nuria Calaf ‡, Pere Casan ‡, Pere J. Riu ‡

†Department of Electronic Engineering. Technical University of Catalonia. Barcelona, Spain.

‡Department of Pneumology. Hospital de la Santa Creu i Sant Pau. Medicine Faculty. UAB. Barcelona, Spain.

Methacholine is an agent that, when inhaled, causes the airways to spasm and narrow if asthma is present. During this test, the patient inhales increasing amounts of methacholine aerosol mist before and after a spirometry test. The methacholine test is considered positive if the lung function drops by 20% . Bronchodilator inhalation follows in case of positive test, until basal state is reached. In this work, 16-electrode EIT measurements were performed on one asthmatic patient the same day he underwent the test, with the own-build TIEsys-4 (Barcelona Group, Spain) as follows.

A. Spirometry was performed on each state: basal, first methacholine dose (MET1), second methacholine dose (MET2), first bronchodilator dose (BRO1), second bronchodilator dose (BRO2). B. Two consecutive EIT measurements followed each spirometry, using the same ventilatory manoeuvre with the patient on a sitting position. Electrodes were placed at the 3rd intercostal space (midclavicular line).

Total image impedance change (IC) was calculated as the sum of all pixel values above 25% of maximum pixel value. Spirometric forced vital capacity (FVC) results were as follows:

	BASAL	MET1	MET2	BRO1	BRO2
V(l)	3.54	3.09	2.77	3.07	3.38
V(%)	100	-13	-22	+11	+22
IC(%)		-13	-21	+15	+24

Where V is air volume measured by spirometry (% V in BRO1 and BRO2 is relative to MET2.) Comparison of percentual increase and decrease of V and IC correlate quite well ($r = 0.998$). Even the amount of decrease/increase was quite similar in both techniques. As the chest expansion did not change significantly during the test, our hypothesis is that reconstructed impedance change is almost completely due to the change in lung air volume, thus suggesting that chest expansion has little impact in the estimated change of impedance. Further measurements on different patients will be performed to confirm this hypothesis and give these results statistical significance.

A method for generating patient-specific finite element meshes for head modelling

Adam Gibson, Martin Schweiger†, Jem Hebden, Simon Arridge†, David Delpy

Dept. Medical Physics and Bioengineering, University College London
†Dept. Computer Science, University College London

Finite element modelling of the head in electrical impedance tomography requires accurate knowledge of the shape of the head. It is not always clinically feasible to obtain this information for every patient, although a limited set of measurements, such as the location of the electrodes, can usually be measured. I will describe a method for warping an existing head-shaped surface to fit a set of measured points on an arbitrary head. This provides a new, individual surface from which a finite element mesh can be obtained. Data simulated from a known head-shaped surface and a generic surface warped to fit the known surface were similar to within experimental errors. However, data generated from a spherical mesh were significantly different from data generated from a mesh of the known surface.

The main application of this work was finite element modelling for optical tomography. In the talk, I will also discuss the similarities between EIT and optical tomography.

Finite element modelling of voltage gradient sensitivity to intra-ventricular bleeding in neonates

R.J. Sadleir

Department of Biomedical Engineering, University of Florida

EIT is a useful method of detecting and quantifying bleeding in difference images. Severe (type III and IV) intra-ventricular bleeding (IVH) in premature infants is associated with mortality, cerebral palsy and post haemorrhagic hydrocephalus. IVH is commonly graded into four types. Type I and II bleeding involves no ventricular distension, and less often results in permanent damage. However, all serious bleeding naturally passes through these classifications. Ultrasound is conventionally used to check for IVH. It is less successful in detecting type I and II cases (only 25-75%) than III -IV and is only usually applied at 6 h intervals. Detection of IVH at stages I or II would be a useful point to alter patient management before ventricular distension and damage occur. Recently, optical tomography results have been published showing that this could be useful in monitoring for IVH. It is also worthwhile to reexamine the application of EIT to this field. Here I present results of 2 and 3D finite element modelling of electric field perturbations resulting from type II bleeding in the neonatal head. The head model included scalp, skull, CSF, brain and blood resistivities. Using an adjacent-current-pair pattern, a maximum relative gradient change of about 2.5% (for an approximate 2.8 ml bleed) and 0.3% (ca. 0.4 ml bleed) was observed in models of bleeding types I and II. Using a polar pattern, the minimum sensitivity required was about two-thirds that indicated using a dipole pattern. The study indicates that monitoring for IVH using EIT may be valuable if artefacts due to shape and electrode resistance changes, as well as CSF flow can be suppressed.

Observation of prompt EIT voltage changes on the human scalp due to brain stimulus

J.C. Murrieta-Lee†, C.J.D. Pomfrett‡, P.C.W. Beatty§, N. Polydorides# , C.B. Mussel†, R.C. Waterfall†and H. McCann†

†Dept. of Electrical Engineering and Electronics, UMIST, Manchester, UK
‡School of Medicine, Univ. of Manchester, UK
§Dept. of Imaging Science and Biomedical Engineering, Univ. of Manchester, UK
Dept of Mathematics, UMIST, Manchester, UK

A pilot experimental study has taken place to investigate the feasibility of imaging human brain function using an EIT system time-locked to an Evoked Response (ER) system. An industrial EIT system was modified to give improved safety and electrical properties, using polar current injection. Sixteen electrodes of the type usually used for EEG monitoring were attached to the scalp and a further two were attached for the purpose of EEG monitoring. In experiments with Visual and Auditory stimuli (VER and AER respectively), short stimuli were applied as single discrete events and, in each case, EIT data acquisition commenced at a pseudo-randomised but pre-determined time in the order of 100ms later, taking 308ms to complete. The time between presentation of successive stimuli was randomised within the range 0.5s – 1.5s. Many frames of data were recorded and compared to data recorded when no stimulus was applied ('reference' frames). We report here on the measured voltage data for two subjects where the injected current was 1mA peak-to-peak at 9.6kHz. The subjects were fully awake.

The reference data yield EIT nearest-neighbour voltage differences over the range 5-28mV. Forward calculations using the simple model and electrical properties given in [1], on the other hand, predicted a voltage range of approximately 15-130mV. The upper limit of the calculated range was found to be very sensitive to the skull conductivity value used in the calculations. In [1], a value of 0.0067 S/m was used for the skull conductivity, but our data favour a value of at least twice that number, and is thus consistent with recent measurements [2,3]. Further optimisation is suggested by varying the conductivity values of the brain, but has not yet been undertaken.

When comparing average EIT frame data taken under stimulus conditions against the reference data, voltage differences of up to approximately 3 mV are observed in both AER and VER cases. Due to their observation very soon after stimulus, we attribute these voltage changes to synaptic activity. The implications in terms of the magnitude of apparent conductivity changes in the brain will be discussed.

1. Towers C M, McCann H, Wang M, Beatty P C, Pomfrett C J D, and Beck M S, 3D Simulation of EIT for monitoring impedance variations within the human head, Physiol. Meas. 21 (2000) 119-124.

2. Oostendorp T.F., Delbeke J. and Stageman D.F., The conductivity of the human skull : Results on in vivo and in vitro measurements, IEEE Trans. Biomed. Eng. 47 (2000) 1487-1492.

3. Akhtari M. et al., Conductivities of three-layer live human skull, Brain Topogr. 14(2002)151-167

Effects of modelling layers and realistic geometry in reconstruction algorithms for EIT of brain function

Adam D. Liston†, Andrew P. Bagshaw‡, Richard H. Bayford†, Andrew Tizzard†, A. Thomas Tidswell§, Hamid Dehghani# and David S. Holder§

†School of Health and Social Sciences, Middlesex University, London.
‡Montreal Neurological Insititute, Montreal, Canada.
§Department of Clinical Neurophysiology, University College Hospital, London, UK
Thayer School of Engineering, Dartmouth College, Hanover, USA

Electrical impedance tomography of brain function has the potential to provide a rapid portable bedside neuroimaging device. Recently, our group published the first ever EIT images of evoked activity recorded with scalp electrodes. While the raw data showed encouraging reproducible changes of a few per cent, the images were noisy. The poor image quality was due in part to the use of a simplified reconstruction algorithm which modelled the head as a homogeneous sphere. The purpose of this work has been to develop new algorithms in which the model incorporates extracerebral layers and realistic geometry, and to assess their effect on image quality.

We considered algorithms incorporating four different forward models of the head: two analytical models i) a homogeneous sphere and ii) concentric spheres in which the brain, skull and scalp were modelled analytically and two numerical (FEM) models iii) a homogeneous, head-shaped volume and iv) a head-shaped volume with internal compartments of contrasting resistivity.

The two analytical sphere algorithms were tested on a) a computer-simulation using the four, concentric spheres model; b) a spherical, electrolyte-filled tank containing a concentric Plaster of Paris shell to mimic the skull. Mean localisation errors for 38 simulated perturbations were 5.82.1mm and 15.96.3mm respectively for four-shell and homogeneous reconstruction. For movement of Perspex along the same axes in the tank, mean localisation errors were 13.7 ± 5.8mm and 20.7 ± 10.1mm. Incorporating shells in the algorithm resulted in peak impedance changes localised more accurately and less centrally than when shells were not included.

All four algorithms were tested on 8 human subjects during between 6 and 12 epochs of exposure to a visual stimulus. Images of visual evoked responses showed no more consistency across subjects with the new algorithms though some individual examples were improved.

Modeling of neuromagnetic field strength outside the human head due to impedance changes from neuronal depolarization

Gershon Ahadzi, Richard Bayford†, Adam Liston† and David Holder

Department of Clinical Neurophysiology and Medical Physics, University College London;
†School of Health and Social Sciences, Middlesex University, London.
Contact email: gershon@madeira.physiol.ucl.ac.uk

The holy grail of neuroimaging would be to have an imaging system which could image the neuronal activity over milliseconds. One way to do this would be by imaging the impedance changes associated with ion channels opening in neuronal membranes in the brain during activity. We have estimated this to be about 1% locally in brain grey matter, recorded at DC. This reduces to about 0.01% if measured at the surface of the head, due to distance and the effect of the resistive skull. In principle, we could measure this using Electrical Impedance Tomography (EIT) as it is close its threshold of detectability. It may be possible to improve signal quality by recording the magnetic field due to injected current with Superconducting Quantum Interference Devices (SQUIDs), used in Magnetoencephalography (MEG).

We have performed a feasibility study by modelling the head as concentric spheres to mimic the scalp, skull, Cerebrospinal Fluid and brain using the Finite Element Method. The magnetic field 1 cm away from the scalp was calculated. An impedance change of 1% in a 2cm-radius volume in the brain was modelled as the region of depolarization . A constant current of 100 μ A was injected into the head from diametrically opposed electrodes.

The standing magnetic field was about 10 pT. The field changed by about 3 fT (0.03%) on depolarization. The noise in a typical MEG system in the frequency band is about 7fT, so this places the change at the limit of detectability. This is therefore similar to electrical recording, as in conventional EIT systems, but there may be advantages to MEG in that the magnetic field directly traverses the skull and instrumentation errors from the electrode-skin interface will be obviated. We plan to compare the signal quality of the electrical or magnetic approach in tank studies.

EEG signal recovery for clinical trials of simultaneous Electroencephalography (EEG) and Electrical Impedance (EIT)

Rebecca Yerworth†‡, Adam Liston†‡, Matthew Sparks, Richard Bayford†‡and David Holder

†Departments of Clinical Neurophysiology and Medical Physics, University College London;
‡School of Health and Social Sciences, Middlesex University, London.
Contact email : rebecca@madeira.physiol.ucl.ac.uk

Diagnosis of neurological conditions such as epilepsy might be enhanced by simultaneous use of the two techniques of EEG (electroencephalography), which measures potentials generated by the brain in the range 1 –100 Hz, and EIT (Electrical Impedance Tomography), which measures those resulting from injected current, usually applied at several tens of kHz. EEG and EIT use different bandwidths, so it might be expected that the use of filters would prevent breakthrough of the EIT signal into the EEG. Unfortunately, the EIT signal saturates the EEG amplifiers, and the switching used in EIT generates subharmonics which are in the EEG bandwidth.

We present a system of passive hardware filters and adaptive software filtering which removes the EIT artefact from the EEG. This has been successfully used in simultaneous EEG and EIT recording on patients undergoing pre-surgery planning for epilepsy; the artefact has been reduced from several hundred μV to less than 5 μV, so that neurologists were happy to use the EEG data for making clinical decisions.

Electro-impedance measurements from women in case of mastalgia

O.Trokhanova†, M.Ohapkin†, A.Karpov‡, V. Cherepenin§, A. Korjenevsky‡

†Yaroslavl State Medical Academy, Russia
‡Clinical Hospital # 9, Yaroslavl, Russia
§Institute of Radio-Engineering and Electronics of Russian Academy of Sciences, Moscow, Russia

Mastalgia declares itself as a pain or discomfort in mammary glands which become severe before menstruation. In the paper we estimated the state of mammary glands through impedance mammography in case of mastalgia and we compared the obtained values with the ones of the normal state and chronic cystic mastitis. We examined 320 women (121 - normal state, 113 - mastitis, 86-mastalgia). To visualize the tissue of a mammary gland we used a 256 channel electro-impedance mammograph. All the women underwent ultrasonic examination of mammary glands and breast radiography. The age of patients was taken into account. An impedance image of the mammary gland in case of mastalgia is shown within a grey scale with smooth transitions from dark to light sections i.e. from low to higher conductivity without foci and where a zone of lactic sinuses is clearly singled out. In corresponding age groups women with mastalgia have the same conductivity in the left and right mammary glands while lying or standing. The values are the same in the first and second phase of a menstrual cycle. You can trace a certain increase of conductivity with age (under $30-0.38\pm0.11$; between 31 and $40-0.39\pm0.12$; between 41 and $50-0.49\pm0.07$). While estimating the graphs in case of mastalgia we can see that an unimodal distribution of conductivity (from 62.2% to 77.2%) prevails. It confirms the absence of focal semeiotics and a diffuse character of involutive processes in the mammary gland. In lying position an average conductivity in age groups with mastalgia “under 30” and “41-50 years” is higher than the one in the normal state (“under 30” - t_{1-2}=3.35, $p<0,01$; “41-50 years” - $t_{1-2}=1.9, p<0,05$) and in group “31-40 years” the electric conductivity in case of mastalgia is lower ($t_{1-2}=2.11, p<0,05$). In a standing position in the group “under 30 years” there is no proved increase in case of mastalgia ($t_{1-2}=1.29, p>0,05$). In group “41-50 years” it’s certainly higher ($t_{1-2}=2.01, p<0,05$) and in group “31-40 years” conductivity is clearly lower ($t_{1-2}=2.29, p<0,05$) than the one in the normal state. During investigations while comparing conductivity in all age groups with chronic cystic mastitis in both positions with the one in case of mastalgia the latter turned out higher (lying position: “under 30 years” – $t_{2-3}=4.92, p<0,01$; “31-40 years” – $t_{2-3}=2.12, p<0,05$; “41-50 years” – $t_{2-3}=2.92, p<0,01$; standing position: “ under 30 years” – $t_{2-3}=3.64, p<0,01$; “31-40 years” – $t_{2-3}=3.63, p<0,05$; “41-50 years” – $t_{2-3}=4.14, p<0,01$).

It proves that mastalgia and chronic cystic mastitis are two different clinical conditions of the mammary gland. The results of our investigations allow us to say that electro-impedance mammography can be used as a method for differential diagnosing the normal state and different clinical conditions of the mammary gland.

Electrical impedance anatomy of the mammary gland

A. Karpov†,O.Trokhanova‡, V. Cherepenin§, A. Korjenevsky§

†Clinical Hospital # 9, Yaroslavl, Russia
‡Yaroslavl State Medical Academy, Russia
§Institute of Radio-Engineering and Electronics of Russian Academy of Sciences, Russia

The mammary gland structure has common features characteristics to the structure of any organ as well as specific ones. A connective tissue capsule, septa and fatty tissue which form a skeleton frame of any organ including mammary glands can be referred to the common anatomic features. A glandular tissue, retromammary fatty tissue and a zone of mammary sinuses which fill the mammary gland skeleton can be referred to the anatomic specific features. In our work we tried to find some anatomic reference points characteristics to the mammary gland in its electrical impedance image. For the analysis we use an electrical impedance image of the mammary gland obtained with the help of a 256-electrode electrical impedance mammograph which had been developed in the Institute of Radio-Engineering and Electronics, Russian Academy of Science. To study an anatomic structure through an electrical impedance method we carried out investigation in the period of maximum functional activity of the organ. For the mammary gland it is the period of lactation. During a layered scanning of the lactating mammary gland we can clearly enough find out its anatomic specific features: retromammary fatty tissue and connective tissue capsule are discovered at a depth of 4-5 cm; formation of septa from the connective tissue capsule begins at a depth of 3-4 cm; septa between mammary gland lobes and glandular tissue are visualized at a depth of 2-3 cm; septa which form the skeleton frame, a glandular tissue and zone of mammary sinuses are relieved at a depth of 1-2 cm. The mentioned above anatomic specific features of mammary gland structure but not so vividly expressed can be seen in electrical impedance mammographs of women of different age in different physiological periods. Understanding of the mammary gland anatomy facilitates understanding of physiological and pathological processes, which occur in the mammary gland.

Variation in breast EIT measurements due to menstrual cycle

Alex Hartov, Nirmal Soni, Keith Paulsen

Thayer School of Engineering, Dartmouth College
alex.hartov@dartmouth.edu

We conducted a study on 8 patients to establish whether periodic changes due to the menstrual cycle will affect EIT measurements on women's breasts. Volunteers were selected from a pool of mammographically normal patients with scattered radiodensity, showing no visible abnormalities on routine mammograms. Each patient came for four visits, scheduled to fall on two time windows in her menstrual cycle, with two visits coinciding with each window, thus covering two cycles or more. The visits were timed so as to fall on phase 1 (days 7 through 14, follicular phase) and phase 2 (days 21 through 28, secretory phase), counting from the last menstrual period. Data were recorded on a single plane for each breast at 10 frequencies. Reconstructed images were produced and zones defined in the resulting data for conductivity and permittivity, corresponding to 75% and 50% of the radius. The data in each zone was averaged and these numbers for three separate frequencies were compared. Using student's t-test of equal means no conclusive differences were found. Three out of eight patients showed a consistent and significant difference at all three frequencies between phase 1 and 2 values for both electrical properties. In five of the eight patients there were significant differences for permittivity in phases 1 and 2. More detailed data will be presented based on more sophisticated analysis at the conference.

Electrical impedance tomography of the breast: comparing normal and abnormal clinical results.

Nirmal K. Soni, Alex Hartov, and Keith D. Paulsen

Thayer School of Engineering Dartmouth College 8000 Cummings Hall Hanover, NH 03755-8000
nirmal@dartmouth.edu

Electrical impedance tomography (EIT) has been used in the recent past for a number of clinical applications. In this work we will present some tomographic and spectroscopic findings for breast imaging from both normal and abnormal cases. The patients were classified normal and abnormal using American College of Radiology (ACR) indexing system for mammograms. The EIT data was collected for 10 discrete frequencies in the range 10kHz to 1Mhz using a single array of 16 electrodes from Dartmouth's generation 1 tomography system. Finite element method was used to reconstruct the images. The images were examined visually and were also compared with mammograms. Dispersion spectra for overall and regional conductivity and relative permittivity were generated. The results were also analyzed based on subject age, body mass index and breast tissue radio-densities.

Feasibility Studies for Electrical Impedance Spectroscopy for Early Tumor Detection

Christina Skourou, P. Jack Hoopes, Keith D. Paulsen

Thayer School of Engineering, Dartmouth College, Hanover, NH, USA Dartmouth Hitchcock Medical Center, Lebanon, NH, USA

Electrical impedance spectroscopy (EIS) has been previously used as a technique for non-invasive assessment of tissue changes. Our prior studies on laboratory animals have also demonstrated the ability of EIS to detect and longitudinally follow tumor growth. This study concentrates on the ability of EIS to detect tumors at a very early stage. Pancreatic DSL-6 tumor cells were inoculated in the biceps femoris muscle of mature male Sprague-Dawley rats. Three to seven days (depending on tumor type) following inoculation, complex impedance measurements were collected both on the tumor implanted and the contra-lateral (non tumor-bearing) legs. The animal was sacrificed immediately after the EIS measurements and tissue beneath the acquisition probe was collected and submitted for H and E stained histology. Microscopic examination of the slides verified the existence of tumors in the measurement field, which co-registered with the EIS findings. In order to verify this information, the study was repeated on a new set of animals using a rat prostate tumor cell line (MLL) and a different strain of rats (Copenhagen). In this study, the tumor implanted leg was also imaged in-vivo using computed tomography (CT) and ultrasound (US) before sacrifice. Although EIS was clearly able to repeatedly detect tumor specific changes, CT and US were not always able to detect early changes induced by the tumor. Microscopic examination of histology slides, once again verified the presence of the tumors. The sizes of these tumors, determined from the histological slides, were measured to be as small as 1.5mm in diameter. The results of this study indicate the potential of EIS to detect changes due to tumor growth at a very early stage even before conventional imaging methods, such as CT or US.

Electrical impedance tomography to differentiate healthy subjects from primary pulmonary hypertension patients.

H.J. Smit, A. Vonk Noordegraaf, P.E. Postmus, P.M.J.M. de Vries, A. Boonstra.

Department of Pulmonology, Vrije Universiteit Medical Center, Amsterdam, The Netherlands.

RATIONALE: Primary pulmonary hypertension (PPH) is a rare disease of the pulmonary vasculature that primarily affects young adults, characterised by sustained elevations of pulmonary-artery pressure, and when untreated with a rapidly fatal course. By means of Electrical Impedance Tomography (EIT), blood volume changes can be visualised and measured, for example in the pulmonary circulation. PPH patients have a strongly reduced functional pulmonary vascular bed, with normal lung function and normal aspect of lung parenchyma on chest X-ray. Together with a-specific symptoms, it can be difficult and take a long time before the right diagnosis is made. In this study we investigated whether the impedance changes in PPH patients differ from the impedance changes in healthy subjects.

METHODS: The Mark I, Sheffield, tomograph was used. Thirty healthy volunteers and twenty-two PPH patients, with normal lung function, participated in this study. The 16 electrodes were equidistantly positioned in the third intercostal space. Subjects lay in supine position, with their arms above their head. Two hundred heart cycles were averaged to obtain one data set. EIT measurements, expressed in arbitrary units (A.U.), were performed in duplicate.

RESULTS: The mean impedance change in the healthy subject group was $215(S.D. \pm 58) \times 10^{-2} A.U.$. The mean impedance change in the PPH group was $81(S.D. \pm 30) \times 10^{-2} A.U.(P < 0.0001)$.

CONCLUSION: Impedance changes in the PPH patients were significantly different compared to the healthy subjects. These results indicate that EIT might be useful as a non-invasive method to diagnose pulmonary hypertension.

Measurement of Velocity and Mass of Moving Structures in Industrial Flows using Electrical Capacitance Tomography

Andrew Hunt, John Pendleton and Malcolm Byars

Tomoflow Ltd. www.tomoflow.com

Electrical capacitance tomography (ECT) is a relatively low resolution measurement, but it has many advantages for industrial use including being non-intrusive, fast and relatively inexpensive. Industrial flows tend to have a large range of materials (solids, gases, liquids) with high contrast in density and electrical properties moving at speeds of up to 10 m/s or more.

In this paper we describe some recent developments of high-speed twin-plane ECT systems and software. These developments include the use of correlation techniques for measurement of industrially important parameters such as the velocity, volume and mass of flow structures in two-component flows, and in particular the mass and velocity of large individual particles, bubbles and groups of particles in solids/gas and gas/liquid flow systems.

Typical ECT flow sensors have between 6 and 12 electrodes placed evenly on the circumference of the pipe, with 5 rings of electrodes along the axial length. Usually rings 1, 3 and 5 are linked as guard electrodes, while rings 2 and 4 are the measurement sets. Measurements can be made at up to 300 complete frames of data per second for 6-electrode twin-plane systems. A large range of sensor shapes and sizes may be fabricated but the most common are circular in cross section with diameters ranging from a few cm to some 10's of cm.

By integrating over specified time periods around flow structures of interest it is possible to measure the volume of individual large particles or clusters of particles. By calibrating mass per unit length of the sensor, these measurements may be expressed directly as particle or cluster mass. Results are presented in the paper for simple gravity-drop flows and also for the conveying of granular material in a pilot plant.

Evaluating electrode position change in an EIT System Using a 3D Finite Difference Model of the Thorax and Direct Human Measurements

Robert P. Patterson and Jie Zhang

University of Minnesota USA

The purpose of this study was to determine how changes in electrode location would influence the EIT image. The study was conducted by changing one electrode location in steps of approximately 0.4 cm in a finite difference model in both the in-plane and out-of-plane direction. Also similar directional changes in a single electrode location were made in one male subject. The EIT images recorded from a male subject used the Sheffield APT System Mark I using 16 electrodes and the associated reconstruction algorithm. The 3D finite difference model of the thorax was constructed from 26 transverse MRI slices 0.5 cm thick gated with the ECG. The model had 225,000 control volumes. The mode was excited in the same manner as done in the Sheffield system and the reconstruction was done using their algorithm.

The Sheffield dynamic system shows an image based on changes with respect to a reference frame. The reference frame was recorded with the electrodes in the standard locations.

The results showed very significant artificial changes, which covered an area from approximately 10% to 35% of the image as the electrode location was varied from about 0.4 to 1.6 cm in the model. Similar results both in area and impedance change were seen in the direct human data. The magnitude of the changes are similar to that observed with various physiological changes.

These results indicate serious problems obtaining absolute resistivities.

Accounting for missing electrode data in electrical impedance tomography

Andy Adler

School of Information Technology and Engineering University of Ottawa, Ontario, Canada
adler@site.uottawa.ca

An unfortunate, but not unusual, occurrence in experimental measurements with Electrical Impedance Tomography, is electrodes which become detached or poorly connected, such that the measured data cannot be used. We propose an image reconstruction methodology which allows use of the remaining good measurements. A finite element model of the EIT dynamic imaging forward problem is linearized as $z = Hx$, where z is the vector change in measurements and x the vector of change in finite element log conductivities. Image reconstruction is represented in terms of a Maximum a Posteriori (MAP) estimate as $x = (H^t(Rn)^{-1}H + (Rx)^{-1})^{-1}H^t(Rn)^{-1}z$, where (') represents the transpose operator, and *Rx* and *Rn* represent the a priori estimates of image and measurement noise cross correlations, respectively. Using this formulation, missing electrode data can be naturally modelled as infinite noise on all measurements using the corresponding electrodes. Simulations were conducted of a small contrasting target at different radial positions as a function of the position of the problem electrode. Contrast position error, point spread function, and total image amplitude were calculated. All values are close (10%) to those calculated without missing electrode data as long as the target was further from the problem electrode than 10% of the medium diameter. When the target was closer than this limit, all error values increased significantly, but the reconstructed image still represented a reasonable "best effort". Application of this technique to experimental data shows similar results. In comparison, simulations were made of the simple approach of setting measurements from problem electrodes to zero. Results show significant errors for targets 25% of the medium diameter from the electrode. The increase in point spread function size above the value for no electrode errors was three times greater for this simple approach than for the MAP estimate.

3D sensitivity distributions with different electrode placement

Mengxing Tang†‡, Wei Wang†, Malcolm McCormick†, Li Wang†, Xiuzhen Dong‡

†3D Imaging and Biomedical Engineering, School of Eng. and Tech., De Montfort Univ., LE1 9BH UK

‡School of Biomedical Engineering, Fourth Military Medical University, Xian, 710032, China

In 3D EIT there are different ways of placing electrodes. How different ways of electrode placement affect the image quality is still largely an open question. This study contributes to the answer of this question by analysing the sensitivity distributions within a cylindrical object when the electrodes are placed in two different ways: plane placement and ring placement. For the plane placement the electrodes are placed on the top of the cylinder. For the ring placement an equal number of electrodes are placed into two rings around the cylinder. A simulation cylinder is made with uniform conductivity distribution. By inserting a perturbation voxel, the sensitivity of the boundary measurements to this perturbation voxel within the cylinder is calculated by Finite Element Method. Then by moving this perturbation voxel, profiles of the sensitivity distribution can be obtained. The results are compared with the two ways of electrode placement. 3D images are also reconstructed by a Gaussian-Newton scheme. The results indicate that the two ways of electrode placement have a similar sensitivity profile. It is also indicated that there is huge differences of sensitivity in different areas within the 3D volume. The reconstructed images correspond well to the sensitivity analysis. Further discussions are given on optimal electrode placement in EIT.

Planar System for Magnetic Induction Impedance Measurement

Claudia H. Riedel, O. Dössel

Institut für Biomedizinische Technik, Universitt Karlsruhe (TH), Germany
Claudia.Riedel@ibt.uni-karlsruhe.de

The measurement of the impedance of biological tissue can deliver data of high diagnostic relevance. The change in the impedance can give important information of the healing process of wounds, biological changes like cancerous growth, nutrient levels, ischemic regions, etc. A contact free method of measuring the impedance of tissue has many advantages e.g. in case of vulnerable tissue like in wounds or in case of tissue covered by a non-conducting layer like the brain.

An oscillating magnetic field, which is produced by a coil, induces eddy currents in a conductive medium. The intensity of these currents depends on the primary field as well as on the conductivity of the tissue. These eddy currents themselves generate an oscillating magnetic field. A secondary coil picks up the resulting field. The induced voltage is analysed in amplitude and phase. Due to an elimination of the primary signal an increase of the resolution can be achieved. This can be done using a gradiometer instead of a single pick up coil.

The reference output of a lock-in-amplifier is used to generate the sinusoidal signal for driving the excitation coil. Because of low magnitude this signal is amplified using a discrete power amplifier. The primary coil is located in between the gradiometer coils. This secondary pair of coils is used to pick up the measurement signal. Two preamplifiers are necessary, because the signal of the gradiometer's output is low and in addition an external reference is generated. The measurement signal itself is detected with the lock-in-amplifier. To measure the impedance in a plane above the tissue, a non-conducting x-y table is used.

First measurements are carried out are using an inhomogeneous phantom.

Keywords: conductivity of tissue, contact-free measurement, coil systems, plane surface measuring, Magnetic induction tomography

Combined Injected and induced current approaches in EIT – a simulation study.

Michal M. Radai, Sharon Zlochiver, Moshe Rosenfeld, Shimon Abboud

In EIT systems current is applied either by injection (Inj.-EIT) or by induction (Ind.-EIT), where in the former and more practiced approach the current is introduced via surface electrodes, and in the latter - via a set of surrounding coils. In both approaches the developed voltages are measured using surface electrodes. There are advantages and disadvantages in each method. For example, in Ind.-EIT only relative conductivity values can be reconstructed, while the spatial distribution of the current can be designed by modifying the coils' geometry. In Inj.-EIT, exact conductivity values can be theoretically retrieved, but the number of independent measurements is limited by the finite number (usually 16 or 32) of the surface electrodes. In this paper we simulate a combined injected/induced EIT system, in order to asses the imaging quality improvement due to the increased number of independent measurements. The simulations were performed using 2D numerical solvers based on the FVM discretization scheme for the forward problem, and the regularized Newton-Raphson iterative algorithm for the inverse problem. Several simple geometries were studied, using various number of excitation coils, injecting electrodes and measuring electrodes. A comparison was carried out among four system configurations:
(1) Six coils Ind.-EIT,
(2) Six injections Inj.-EIT,
(3) Combined injected/induced EIT with 6 coils and 6 injections (a total of 12 measurements), and
(4) Combined injected/induced EIT with 3 coils and 3 injections (a total of 6 measurements).

An expected imaging quality improvement was found in the third configuration: the Inj.-EIT measurements contributed in reconstructing true conductivity values, while the Ind.-EIT contribution was expressed in the smoothness of the reconstruction. More interestingly, an unexpected improvement was found in the fourth configuration (where half of the measurements were taken from the Inj.-EIT and half from the Ind.-EIT), which may be explained by a synergetic added value of the combination.

MIT image reconstruction based on edge preserving regularization.

R. Casanova, A. Silva, A.R. Borges

Instituto de Engenharia Electrónica e Telemática de Aveiro - IEETA Universidade de Aveiro

Image reconstruction in electrical tomography is a non-linear and ill-posed inverse problem. This kind of problem is usually approached through the use of regularization theory and the introduction of a priori information about the solution. EIT image reconstruction literature offers multiple examples of papers based on Tikhonov regularization, Conjugate gradient, Landweber iteration, etc. This kind of techniques, however, tends to produce blurred images due to the fact that discontinuities are strongly penalized. Recently, a lot of interest has been devoted to methods with edge preserving properties, like those related to total variation, wavelets and half-quadratic regularization.

Image reconstruction using regularization techniques has been less explored in MIT than in ERT or ECT. In the present work the performance of an edge preserving regularization method called ARTUR is evaluated. ARTUR is a deterministic method based on half-quadratic regularization. A priori information is introduced through the use of a non-negativity constraint which is incorporated in the algorithm. The framework used to test the method is an analytical model that generates projection data given the position, the radius and the permeability of a cylindrical and nonconductive object.

Results are quite encouraging. It is shown that even in the presence of strong gaussian additive noise, the method is still able to recover the main features of the object. It is also shown how significant is the introduction of non-negativity constraining in the reconstruction.

This work was financially supported by a grant from FCT(Portugal) - Fundao para a Ciencia e Tecnologia- Servio de Recursos Humanos.”

Sensitivity maps for magnetic induction tomography (MIT): Low-contrast perturbations in a background with physiological conductivity.

H. Scharfetter, K. Hollaus, R. Merwa

Introduction: The inverse problem of magnetic induction tomography (MIT) is different from that for EIT because of the occurrence of both the electrical scalar and the magnetic vector potential. In order to understand the inverse problem, a careful analysis of the sensitivity maps has to be carried out for perturbations within conducting objects.
Method: We calculated sensitivity maps for a single MIT-channel and a cylindrical tank (diameter 200 mm) with a spherical perturbation (diameter 50 mm) and with conductivities in the physiological range (0.4 vs. 0.8 S/m). As excitation coil solenoids with 2 different diameters (30 mm and 100 mm) were simulated. 2 planar gradiometers (PGRAD) with different coil diameters (30 mm and 50 mm), coaxial receiver coils (CRC) with 15, 30 and 50 mm diameter and a coaxial planar gradiometer (CPGRAD) were considered. The axis of the coil system was perpendicular to the cylinder axis. A finite element model with edge-elements (magnetic vector potential) and nodal elements (electrical scalar potential) was applied.
Results: The sensitivity maps depend little on the diameter of the excitation coils. The dependence on the receiver coil type is very pronounced. CRC: The sensitivity is lowest along the coil axis, increasing dramatically with the distance from the coil axis. The maps depend little on the diameter of the coils. PGRAD: The sensitivity is zero on the coil axis, exhibiting a complex pattern with a strong increase of the sensitivity with the distance from the coil axis. CPGRAD: The sensitivity map is symmetrical with respect to the coil axis and shows again a strong increase towards the periphery. The results for the CRC and the PGRAD are in good agreement with previously published measured data.
Discussion: Sensitivity maps for near-physiological MIT-measurements are shown for the first time and should provide the basis for solving the inverse problem of MIT. All maps have in common a minimum sensitivity on the coil axis and are therefore completely different from those for isolated objects in the empty space and from those known in EIT.

A primary field compensation scheme for planar array magnetic induction tomography

S Watson†, R J Williams†, H Griffiths‡and W Gough§

†School of Electronics, University of Glamorgan, Pontypridd, CF37 1DL, UK, swatson1@glam.ac.uk
‡Department of Medical Physics and Clinical Engineering, Singleton Hospital, Swansea SA2 8QA, UK
§Department of Physics and Astronomy, Cardiff University, Cardiff CF2 3YB, UK

Magnetic induction tomography (MIT) systems for biomedical applications described in previous publications have been required to operate in the frequency range of 10 - 20MHz to achieve sufficient measurement precision for the imaging of samples with conductivities in the biological range. High excitation frequencies, and a limitation of the operating frequency range, may not however be optimal for acquiring clinically useful data.

Measurement precision may be improved by incorporating some form of primary field compensation / cancellation scheme. Schemes which have been described previously include gradiometric approaches and the use of 'back-off' coils. In each of these methods however, the primary field cancellation is achieved only for a single transmitter / receiver combination. For the purpose of imaging it would be desirable for a fully electronically scanned MIT system to provide a complete set of measurements, all with the primary field cancelled

A single channel suitable for incorporation into such an MIT system with planar-array geometry is described. The transmitter is a 6 turn coil of wire 5 cm in diameter. The receiver is a surface mount inductor, of inductance 10 microH, mounted such that, in principle, no primary-field flux threads it.

The results of measurements carried out with the single channel system suggest that the signal due to the primary excitation field can be reduced on average by a factor of 78 by the sensor geometry over the operating frequency range 1 - 10MHz. The standard deviation and drift of the signal with the system adjusted for maximum primary field cancellation, expressed as a percentage of the signal with the receiver coil rotated for maximum sensitivity to the primary field, was 0.003% and 0.02% respectively. The filter time constant used was 30ms.

Non-invasive measurement of liver iron overload by magnetic induction using a planar gradiometer

J. Rosell†, R. Casañas †‡, A. Altes§, R. Merwa#, K. Hollaus# and H. Scharfetter#

†Departament d'Enginyeria Electrnica, Universitat Politècnica de Catalunya, 08034 Barcelona, Spain.
‡Escuela de Bioanálisis, Facultad de Medicina, Universidad Central de Venezuela, Caracas, Venezuela.
§Departamento de Hematologia, Hospital de la Santa Creu i Sant Pau, Barcelona, Spain.
Institute for Biomedical Engineering, Technical University Graz, 8010 Graz, Austria.

Introduction: The measurement of hepatic iron overload is of particular interest in cases of hereditary hemochromatosis or in patients subject to periodic blood transfusion. The measurement of plasma ferritin provides an indirect estimate but the usefulness of this method is limited by many common clinical conditions (inflammation, infection, etc.). Liver biopsy provides the most quantitative direct measurement of iron content in the liver but the risk of the procedure limits its acceptability. Non-invasive measurement techniques studied up to now are MRI and magnetic susceptometry. Magnetic susceptometry systems are based on SQUIDs and the main problem is the need of a cryogenic region and a special screened room. This work studies the feasibility of a magnetic induction (MI) low-cost system to measure liver iron overload.
Methods: We adapted the dimensions of a previously developed experimental MI system, used for in-vitro measurements, for non-contact and non-invasive human measurements. The excitation field is produced by a coil with a current of 20 App at 28 kHz. The detection coil is a planar gradiometer. We measured 10 patients and 8 volunteers. The subject was moved in a plane parallel to the gradiometer several times to measure the repeatibility. The real and imaginary parts of DB/B0 were measured. Plastic tanks filled with water, saline and ferric solutions were measured for calibration purposes. Theoretically, the detected real part is proportional to the permittivity (e) and the permeability (m) and the imaginary part is proportional to the conductivity (s). We used a FEM model and an eddy current solver to evaluate the experimental results.
Results: The results for water show no significant imaginary component and a negative real part due to the water's diamagnetism. Measuring saline tanks we increased the imaginary component as expected. For measurements in humans we observed a positive real part. This could be attributed to a paramagnetic object or to the effect of the permittivity. FEM models show that the main contribution is the permittivity.
Discussion: The contribution of the permittivity is stronger than the contribution due to the increase in permeability produced by iron stores in the liver. The different frequency behaviour of these two components on the detected real part of DB/B0 may be used to separate both contributions. Furthermore, the effect of other structures (tissues) in the abdomen will require a more precise modelling of the body in order to make possible the quantitative measurement of liver iron content.

Preliminary Results of Dartmouth's high frequency EIT System

Ryan Halter, Alex Hartov, Keith Paulsen

Thayer School of Engineering Dartmouth College

We have recently completed the final implementation of a new high frequency DSP based EIT system to be used in a clinical setting in order to investigate the merits of electrical impedance imaging as a breast cancer screening methodology. The system has spectral outputs ranging from 10kHz to 10MHz and is capable of applying spatially varying voltage patterns to electrodes arranged in four planes of 16 radially positioned electrodes. Implementing the system involved the design of a new patient interface, system calibration, phantom studies and preliminary patient images. Several patient interface design changes were made to our previous system in order to accommodate the new design. The use of a more robust radially translating electrode system to improve patient interfacing, close proximity of drive and data acquisition circuit boards to the electrodes to reduce losses due to high frequency signal transmission characteristics, and the use of multiplane electrode rings for 3D imaging will be discussed. System calibration was realized through use of a digital multimeter to DC reference a single channel. The remaining channels were then calibrated with respect to this reference channel. Both 2D and 3D images using the new 3D data acquisition scheme were obtained for various phantom experiments. Finally, preliminary patient images will be presented.

Simultaneous recording of EEG signals during EIT measurement

Sunao Iwaki †,§, Giorgio Bonmassar†, Itzhak Aharon†, Michael Lev‡, John W. Belliveau†

†NMR Center, ‡Dept. of Radiology, Massachusetts General Hospital, §National Institute of Advanced Industrial Science and Technology

Introduction: In this study, we introduced high-precision data acquisition system to measure electroencephalographic (EEG) signals as well as the voltage distribution used for electrical impedance tomography (EIT).

Methods: Eighteen electrodes, two of which were the 'stimulating' electrodes, were attached in the transverse plane of the subject's head. White noise with maximum voltage of 1V was applied as an injecting current. EIT signals in conjunction with EEG components were measured at 8 neighboring electrode pairs and sampled using high-precision A/D converter with a sampling rate of 100kHz.

Phantom Experiment: First, we conducted a phantom experiment, in which cylindrical insulator was placed in the cylindrical conducting medium. We observed changes in the EIT signals up to about 8 % as we move the insulator. EEG Recording under EIT Measurement: We measured the EIT/EEG signals during subjects repeating 30 s of eyes open followed by 30 s eyes closed. Increased alpha-band (8-13 Hz) activities in the frequency domain were detected during the 'eyes-closed' period, and the alpha-band components were observed in the time-domain EIT/EEG signals during 'eyes-closed' period after 40Hz low-pass filtering.

Discussion: The results obtained so far show that we are able to record spontaneous EEG activities during EIT measurement. As we use white noise for the injecting stimuli, it may be possible to record event-related EEG components with adequate signal averaging. This system will also allow us to measure EIT signals inside the MRI scanner using specialized electrodes and the adaptive noise elimination technique, which will provide the additional information about the relationship between the changes in impedance and the hemodynamic response in the brain.

Feasibility of the UCLH Mark II EITS system for imaging stroke : tank and modelling studies

RJ Yerworth, L Enfield, RH Bayford†and DS Holder

Department of Clinical Neurophysiology and Medical Physics, University College London;
†School of Health and Social Sciences, Middlesex University, London.
Contact email : rebecca@madeira.physiol.ucl.ac.uk

Recently, thrombolytic "clot-busting" treatment for stroke has become available. It can lessen the damage due to stroke by dissolving blood clots in arteries to the brain but must be given within three hours. It is essential to perform a brain scan first to decide if the stroke is due to blockage of an artery or bleeding; thrombolytic agents must not be given if there is bleeding, as they can make it worse. Unfortunately, many eligible cases cannot receive this treatment because access to a scanner is not immediately available. EIT has the potential to overcome this bottleneck by providing urgent brain imaging and discrimination of these conditions. Until now, clinical EIT studies of brain function have been performed by recording changes over time at a single frequency; this application requires single "one-off" images. We propose to produce these using the UCLH Mark II EIT spectroscopy system. The feasibility of this application has been assessed using a saline filled tank in which biological test samples were imaged from 1 – 500 kHz using the UCLH Mark II EITS system, and by analysis of data from the literature of the impedance changes in the brain caused by haemorrhagic or ischaemic stroke. The theoretical analysis indicates that impedance contrasts of –30% or +20% relative to normal brain may be expected due to haemorrhage or acute ischaemic stroke, and that changes of this size may be imaged in tanks with a signal-to-noise ratio of better than 10 to 1. Image quality is usually less in clinical than in tank studies, but this supports the belief that EITS may be able to provide images of a suitable quality for clinical use; a clinical trial is in progress.

OXBACT5 -a progress report on a modular multiple-source data acquisition system (DAS) for EIT.

Chris McLeod, Dimitar Kavalov and Alex Yue,

Oxford Brookes University, UK.

We reported the development of OXBACT5 in August 2002 during the First Mummy Range EIT Workshop. Since then we have continued the development and, at the risk of some repetition for some attending the conference, will report on the structure and specifications.

The patient interface has to be suitable for use in intensive care so electrode placement has to be speedy and the determination of electrode position made simple. The DAS has to be small as there is little room around such patients and nursing needs take priority. The link between the DAS and the host computer will be wireless for the same reason.

The basic DAS module is built around a Xilinx Virtex-II FPGA which sits on a standard PCIbus interface. Multiple modules can therefore be stacked for a larger system. Each module controls 16 programmable current sources and 64 voltage measurement circuits. Up to 15 current patterns can be applied per image frame and a frame rate of 25/second has been specified.

The host computer interface is in MATLAB, controlling the DAS and the reconstruction process and presenting the reconstructed images. It is intended that this hardware and software interfacing will make the system accessible for other research groups.

Black-box Algebraic Multigrid for the 3D Forward Problem arising in Electrical Resistance Tomography

Manuchehr Soleimani, Catherine Elizabeth Powell

Department of Mathematics, UMIST, Manchester, M60 1QD
m.soleimani@umist.ac.uk
cp@fire.ma.umist.ac.uk

Image reconstruction in Electrical Resistance Tomography (ERT) is an ill-posed non-linear inverse problem. In most solution schemes for the image reconstruction, the forward problem plays a major role. For example, an iterative solution scheme requires the solution of a linear forward problem at each step. The discretisation of the inner problem via nodal or edge based finite element techniques is well understood. However, the resulting large, sparse systems of equations generally have large condition numbers; their solution is non-trivial. Moreover, the speed of solution of the forward problem can have a significant impact on solution efficiency. Fast and robust solvers are therefore essential.

We discuss the application of black-box algebraic multigrid AMG to the symmetric linear systems of equations arising from two finite element discretisations of the 3D forward problem. In this approach, AMG is used as a preconditioner, accelerated by Krylov subspace methods such as CG or BICGSTAB. Set-up only needs to be performed once. Unlike conventional approaches based on incomplete factorisation methods, no parameters need to be *tuned* by the user. AMG is applied as a black-box.

Numerical results are presented to illustrate the robustness and speed of the scheme. We demonstrate that the AMG scheme can significantly reduce the total computational cost of the image reconstruction problem.

An idea about utilizing bulk volume fraction information in local volume fraction estimation

Lasse M. Heikkinen, Robert M. West and Marko Vauhkonen

Lasse M. Heikkinen and Marko Vauhkonen are with Applied Physics, University of Kuopio, P.O.Box 1627, FIN-70211 Kuopio, Finland
Robert M. West is with Nuffield Institute for Health, University of Leeds, LS2 9JT, UK

For many industrial processes the volume fraction of the one phase such as gas or solid can be of considerable importance. For this reason it is often controlled within certain limits and therefore is known at least vaguely. Tomographic imaging of volume fraction can provide very valuable information not only of the bulk volume fraction but also of the spatial distribution of the phase of interest. Prior information about the bulk volume fraction can assist in tomographic inversion, even if this information is not precise. In this presentation we will give an idea how bulk volume fraction information can be taken into account in tomography based local volume fraction estimation. ¿From the mathematical point of view the bulk volume fraction is a volume integral of the spatial distribution of the phase of interest with respect to spatial coordinates. This prior information can be include in the inversion as a side constraint. A simple illustrative 2D example is used to demonstrate the method. The example is considered from the statistical point of view. Also possible applications are briefly introduced.

Use of Reconstruction Bases in Electrical Impedance Tomography

Hamid Dehghani, Nirmal Soni, and Keith D Paulsen

Thayer School of Engineering, Dartmouth College, Hanover, NH 03755, USA
Hamid.Dehghani@dartmouth.edu

Image reconstruction in Electrical Impedance Tomography (EIT) is achieved numerically by minimizing an objective function, which depends on the difference between measured and calculated data. While the forward solver (used to generate the calculated data) can take the form of either numerical or analytical models, most non-linear quantitative reconstruction algorithms require an iterative method, through which images of internal electrical property distributions can be reconstructed. In most algorithms the internal properties are varied on the same bases as the forward (field) solution, often leading to an under-determined problem. We are concerned with accurate imaging of the female breast, in order to identify and characterize suspicious anomalies; therefore, quantitatively accurate reconstructed images are essential. In this work, we will discuss the use and application of various reconstruction bases, in particular, alternative mesh, pixel and region bases, and will show their advantages in both speed and accuracy. Finally, we will show and present results from experimental studies, where image-driven-region bases are used to provide both quantitatively and qualitatively reconstructed images.

A Two-phase Electrical Impedance Tomography Algorithm using the Extended Kalman Filter

R.G Lima, F.C. Trigo, M.B.P. Amato

University of Sao Paulo, Brazil.

Electrical Impedance Tomography (EIT) estimates the resistivity (or conductivity) field within a body when a low amplitude current pattern is applied to its boundary surface and the potential at determined points of that surface is measured through electrodes or, alternatively, when a potential is applied and the current flowing through the surface is measured. In this work, we use the extended Kalman filter to estimate time-varying resistivity distribution in EIT. The domain with unknown continuous resistivity distribution is modeled through the Finite Element Method (FEM), generating a finite-dimensional model representing a section of a human thorax at middle-lung level. A discrete-time state-space observation model is obtained from the FE equations; a random-walk model represents the behavior of the pulmonary system. Tunning Kalman filter for simultaneous estimation of electrode contact impedances and impedance distribution is a more complex task than using a two-phase identification procedure. A two-phase identification procedure alternates electrode contact impedances estimation and resistivity distribution estimation. The method is shown to be convergent using the fixed point contraction mapping theorem. Numerical simulations and experimental results are presented.

Recent Developments in Reconstruction Algorithms in EIT

W.R.B. Lionheart

Department of Mathematics, UMIST, Manchester

To a large extent the standard method of solving the inverse problem in EIT, in geophysics, medicine and process monitoring, is to use Gauss-Newton method to minimize

$$||V(\sigma) - V_{\text{meas}}||^2 + R(\sigma)$$

where $V(\sigma)$ is the vector of voltage data, σ a disceretized conductivity, and R a regularization term, typically a quadratic function. The forward solution, and the calculation of the Jacobian, is achieved using the finite element method. Assuming the measurement errors are independent and normally distributed with the same variance, this approach gives the maximum of the posterior distribution given a prior determined by R.

The simplest prior assumes a specified degree of smoothness on σ. In the ideal case we would represent all our a priori information in the prior distribution, carefully model the error distribution and calculate the posterior using for Markov Chain Montecarlo method [1]. Although this is very computationally demanding.

Intermediate approaches use simple but realistic a priori information such as bound constraints [2] and total variation regularization [3]. Knowing that the conductivity takes only two values (a two phase problem) is an important special case which can be treated by the monotonicity method [4], or by linear sampling method [5].

An extreme but fruitful approach to regularization is to fit a parameterized anatomical model.

Scattering transform methods [6] provide a hope of a direct non-linear reconstruction algorithm, although this has not been generalized to 2D nor is it clear how to introduce a priori information directly.

References

1. S Meng, Markov chain Monte Carlo techniques and spatial-temporal modelling for medical EIT, this conference
2. Polydorides, N, Image Reconstruction for Soft Field Tomography, PhD Thesis, UMIST, 2002. `http://www.ma.umist.ac.uk/bl/theses/`
3. Borsic A, McLeod C N and Lionheart W R B 2001 Total variation regularisation in EIT reconstruction 2nd World Congr. on Industrial Process Tomography (Hannover), See also A Borsic PhD Thesis, Oxford Brookes University 2002
4. A Tamburrino and G Rubinacci, A new non-iterative inversion method for electrical resistance tomography, Inverse Problems 18, 2002 1809-1829
5. D Colton, H Haddar, P Monk, The Linear Sampling Method for Solving the Electromagnetic Inverse Scattering Problem, preprint: `http://www.math.udel.edu/ monk/`
6. J. Mueller and S. Siltanen, Direct Reconstructions of Conductivities from Boundary Measurements, SIAM J. Sci. Comput. 24, 2003, pp. 1232-1266

Markov chain Monte Carlo techniques and spatial-temporal modelling for medical EIT

Sha Meng

Department of Statistics, University of Leeds

Many imaging problems can be shown to be inverse problems: that is either there is no unique solution or the solution does not depend continuously on the data. As a consequence solution of inverse problems based on measured data alone is unstable, particularly if the mapping between the solution distribution and the measurement is also nonlinear. To deliver a practical stable solution it is necessary to make considerable use of prior information or regularisation techniques. The role of a Bayesian approach is therefore of fundamental importance, especially when coupled with Markov chain Monte Carlo (MCMC) sampling to provide information about solution behaviour and deal with many highly nonlinear inverse problems. As for priori information, spatial smoothness has been well justified for many applications of image to produce improved reconstruction. In the medical EIT example considered here, however, nonlinearity increases the difficulty of imaging using only boundary data. Visualizations can have artifacts including blurring, masking, shadowing and distortions. Therefore an evolution model is incorporated to gain benefit from temporal smoothing with the balance between spatial and temporal components changing with time. There are many potential applications, such as, in medical EIT imaging, detection and classification of tumours, monitoring of pulmonary and cardiac functions; in industrial process EIT, on-line monitoring and control of evolving processes. A simulation example is considered where the aim is to monitor the progress of tumour growth and to assess the effect of surgical intervention.

Reconstruction of Current Density and Conductivity Distributions using One Component of Magnetic Flux Density

Ohin Kwon†, Jin Keun Seo‡, Byung Il Lee§and Eung Je Woo§

†Department of Mathematics, Konkuk University, Korea
‡Department of Mathematics, Yonsei University, Korea
§Department of Biomedical Engineering, Kyung Hee University, Korea

Magnetic Resonance Current Density Imaging (MRCDI) is to provide current density images of a subject using an MRI system with a current injection apparatus. The injection current generates a magnetic field that we can measure from MR phase images. We obtain internal current density images from the measured magnetic flux densities via Ampere's law. In Magnetic Resonance Electrical Impedance Tomography (MREIT), we use the magnetic flux density and/or current density data in addition to boundary voltages to reconstruct cross-sectional conductivity images. However, in both techniques, we must rotate the subject to acquire all of the three components of the induced magnetic flux density. This subject rotation is impractical in clinical MRI systems when the subject is a human body. In this paper, we propose new methods to eliminate the requirement of subject rotation. In our new techniques, we need to measure only one component of the induced magnetic flux density and reconstruct both cross-sectional resistivity and

Three-Dimensional Forward Solver for Magnetic Resonance Electrical Impedance Tomography (MREIT) using Recessed Electrode

Eung Je Woo†, Byung Il Lee†, Suk Hoon Oh†, Soo Yeol Lee†, Min Hyeung Cho†, Ohin Kwon‡and Jin Keun Seo§

†Department of Biomedical Engineering, Kyung Hee University, Korea
‡Department of Mathematics, Konkuk University, Korea
§Department of Mathematics, Yonsei University, Korea

In Magnetic Resonance Electrical Impedance Tomography (MREIT), we try to reconstruct a cross-sectional resistivity (or conductivity) image of a subject. When we inject a current through surface electrodes, it generates a magnetic field. Using a Magnetic Resonance Imaging (MRI) scanner, we can obtain the induced magnetic flux density from MR phase images of the subject. We use recessed electrodes to avoid undesirable artifacts near electrodes in measured magnetic flux densities. An MREIT image reconstruction algorithm produces cross-sectional resistivity images utilizing the measured internal magnetic flux density in addition to boundary voltage data. In order to develop such an image reconstruction algorithm, we need a three-dimensional forward solver. Given injection currents as boundary conditions, the forward solver described in this paper computes voltage and current density distributions using the finite element method (FEM). Then, it calculates the magnetic flux density within the subject using the Biot-Savart law. The performance of the forward solver is analyzed and found to be enough for use in resistivity image reconstructions and also in the experimental design and verification.

Introduction to MR-EIT and Review of Reconstruction Algorithms

Y. Ziya İder† B. Murat Eyüboğlu ‡

† Department of Electrical and Electronics Engineering, Bilkent University, Ankara, Turkey
‡ Department of Electrical and Electronics Engineering, METU, Ankara, Turkey

Magnetic Resonance – Electrical Impedance Tomography (MR-EIT) has first been proposed in 1992. In addition to peripheral voltage measurements it makes use of the measurements of the internal magnetic field generated by the internal current density distribution. Magnetic field is measured by using MRCDI techniques (Magnetic Resonance Current Density Imaging) inside an MRI system while current is injected to a conductive object. Specially designed MR pulse sequences are used for this purpose. Phase unwrapping techniques must be utilized to extract the magnetic field from the MR phase images. Once the magnetic field is measured, internal current density is calculated by taking the curl of the magnetic field. MR-EIT algorithms fall into two categories; those utilizing the magnetic field measurements directly (H-based algorithms), and those utilizing internal current density information derived from magnetic field measurements (J-based algorithms). The latter class of algorithms suffer from the need for measurement of all three components of the magnetic field because calculation of current density by the curl operation requires all of these three components. This necessitates the rotation of the object into all Cartesian axes in the MRI system. On the other hand, algorithms have been proposed which aim at utilizing only one component of the magnetic field directly. This paper introduces the MR-EIT problem, measurement techniques, and also the various reconstruction algorithms proposed so far. The reconstruction algorithms to be discussed are the methods based on fitting the peripheral voltage measurements to those calculated by integrating the electric field inside, methods utilizing construction of equipotential lines, methods based on minimizing the difference between measured and calculated current densities, methods based on sensitivity matrices, methods based on formulating the problem as a set of first order partial differential equations and others. The methods are introduced briefly in order to emphasize their differences with respect to several criteria. These criteria are based on the following questions: Are the methods iterative or direct? What combination of peripheral voltages and magnetic field measurements is used? Are the methods applicable to 2D and 3D reconstruction as well as slice and field-of-view imaging? Do the methods have well established uniqueness conditions? Are they J-based or H-based with single component of H measured? In addition to reviewing the state-of-art in MR-EIT, identification of new areas of investigation will be attempted.

Combined Use of MRCDI and MR-EIT for Lead Field Imaging

B. Murat Eyüböğlu and Orçun Özbek

Department of Electrical and Electronics Engineering, Middle East Technical University, Ankara - Turkey
E-mail:meyub@metu.edu.tr

Externally applied electric current flow inside a volume conductor can be imaged using Magnetic Resonance Imaging. Combining current density information with EIT surface potential measurements, it is also possible to reconstruct high resolution conductivity images of a volume conductor. These two emerging imaging technologies are known as Magnetic Resonance Current Density Imaging (MRCDI) and Magnetic Resonance - Electrical Impedance Tomography (MR-EIT).

Sensitivity of certain current injection - voltage masurement strategy to local conductivity in EIT, and sensitivity of an EEG or ECG leads to bioelectric sources can be described by the lead field phenomena. Lead field of a certain current injection pattern or potential measurement lead can be imaged using MRCDI and MR-EIT images. Then, lead field information can be used to calculate sensitivity of a given current injection - voltage masurement strategy to conductivity distribution in EIT or sensitivity of measurement electrodes to dipole sources in EEG and ECG recordings. In this study, MRCDI technique is implemented to obtain lead fields and sensitivity maps on several experimental phantoms with embedded conductor and insulator objects, using 0.15T METU-MRI system.

Magnetic Resonance - Electrical Impedance Tomography (MR-EIT) using Magnetic Flux Density in One Direction and Experimental Realisation

Özlem Birgül†, B. Murat Eyübŏglu†and Y. Ziya İder

†Department of Electrical and Electronics Engineering, Middle East Technical University, Ankara - Turkey
+Department of Electrical and Electronics Engineering, Bilkent University, Ankara - Turkey
E-mail: meyub@metu.edu.tr

Magnetic Resonance - Electrical Impedance Tomography (MR-EIT) is an emerging imaging technique, that reconstructs electrical conductivity images using magnetic flux density measurements acquired employing MRI together with conventional EIT measurements. A reconstruction algorithm based on the sensitivity matrix relation between conductivity and magnetic flux density is preferred. This algorithm uses only one component of the magnetic flux density distribution and the requirement of object rotation is eliminated. Once the relative conductivity distribution is found, it is scaled using the peripheral voltage measurements to obtain the true conductivity distribution. In this study, MR-EIT technique is implemented using 0.15T METU-MRI system. Reconstructed images of several experimental phantoms, constructed using insulator and conductor objects in saline solution, will be presented.

Equipotential Projection Based Magnetic Resonance - Electrical Impedance Tomography (MR-EIT) and Experimental Realisation

B. Murat Eyüböğlu and Mahir S. Özdemir

Department of Electrical and Electronics Engineering, Middle East Technical University, Ankara - Turkey
E-mail: meyub@metu.edu.tr

Abstract: Magnetic Resonance - Electrical Impedance Tomography (MR-EIT) is an imaging modality, which is developed to produce images of true conductivity with high resolution, utilizing current density distribution and peripheral potential measurements induced by an externally applied current. Current density distribution can be imaged using Magnetic Resonance Current Density Imaging (MRCDI) techniques. Based on the fact that isocurrent lines are perpendicular to isopotentials, potentials measured at the surface are projected into the field of view along the equipotential lines and potential gradient is found. Conductivity images are reconstructed utilizing the potential field gradient and the current density distribution with millimeter spatial resolution and high quantitative accuracy. Sensitivity of MRCDI measurements to internal regions is uniform, since the measurements are made for the entire object. Spatial resolution is also independent of position and in the order of a few millimeters. We will present the results of performance tests on simulated data and the images obtained from experimental phantoms performed on 0.15 Tesla METU-MRI system.

Method of Characteristics for Reconstruction in MR-EIT formulated as a system of First Order Hyperbolic Partial Differential Equations

William R.B. Lionheart† Y. Ziya İder‡ Serkan Onart‡

† Department of Mathematics, UMIST, UK
‡ Department of Electrical and Electronics Engineering, Bilkent University, Ankara, Turkey

In injected current MR-EIT (Magnetic Resonance - Electrical Impedance Tomography) current is injected by surface electrodes and the magnetic field intensity generated by the internal current distribution is measured. Measurement of the magnetic field intensity **H** inside the object is achieved by a Magnetic Resonance Imaging system using a specially designed pulse sequence. Internal current density **J** is then calculated using the differential form of Ampere's Law i.e. $\mathbf{J} = \nabla \times \mathbf{H}$. From the information on the internal current density distribution, conductivity (or resistivity) distribution of the object is reconstructed. In this study the resistivity reconstruction problem of MR-EIT is formulated as a system of first order hyperbolic partial differential equations. In these equations log-resistivity is the system variable and the components of the measured internal current density form the coefficients of the hyperbolic equations. The numerical solution of these equations is achieved using the method of characteristics. This requires the specification of Cauchy data on a non-characteristic surface, which is sufficient to reconstruct log-resistivity on the characteristic curves intersecting the non-characteristic surface. The method is applicable to full 3D reconstruction as well as to slice imaging of 3D objects and also to FOV (field of view) imaging. The method is a direct method as opposed to an iterative one. It is shown that if two or more current injection profiles are used such that internal current density vectors due to at least two different current injection profiles are not aligned in a certain subset of the object, then unique reconstruction can be achieved up to an unknown multiplicative constant. This constant is then found using a single voltage measurement on the periphery of the object. Simulation studies are undertaken to demonstrate the implementation of the method for 2D objects.

Finite Difference and Gradient Based solutions for MR-EIT formulated as a system of First Order Hyperbolic Partial Differential Equations

Y. Ziya İder† William R.B. Lionheart‡ Serkan Onart†

† Department of Electrical and Electronics Engineering, Bilkent University, Ankara, Turkey

‡ Department of Mathematics, UMIST, UK

In injected current MR-EIT (Magnetic Resonance - Electrical Impedance Tomography) current is injected by surface electrodes and the magnetic field intensity **H** generated by the internal current distribution is measured. Measurement of the magnetic field intensity inside the object is achieved by a Magnetic Resonance Imaging system using a specially designed pulse sequence. Internal current density **J** is then calculated using the differential form of Ampere's Law, i.e. $\mathbf{J} = \nabla \times \mathbf{H}$. From the information on the internal current density distribution, conductivity (or resistivity) distribution of the object is reconstructed. The resistivity reconstruction problem of MR-EIT can be formulated as a system of first order hyperbolic partial differential equations, where log-resistivity is the dependent variable. In this study the numerical solution of these equations is achieved using two approaches. In the first approach gradient of log-resistivity is calculated at each point in the object and log-resistivity is obtained by simple integration. This approach is useful in establishing the uniqueness conditions. It is shown that, at all points in the object, gradient of log-resistivity can be calculated provided that at each point there are at least two non-aligned current vectors corresponding to two different current injection patterns. The second approach is based on obtaining a Finite Difference approximation of the hyperbolic partial differential equations. This approach has the advantage of incorporating regularization techniques in the algorithm. The methods described are direct (non-iterative) and are applicable to 2D and 3D reconstructions as well as slice and FOV (field of view) imaging. Numerical simulations are presented to demonstrate implementation aspects of the algorithms.

A new Iterative Reconstruction Algorithm for MR-EIT using the Laplacian of one component of Magnetic Field Intensity

Serkan Onart, Y. Ziya İder

Department of Electrical and Electronics Engineering, Bilkent University, Ankara, Turkey

In MR-EIT there are several algorithms to reconstruct cross-sectional resistivity images by using internal current density distribution **J** which is obtained by taking the curl of the magnetic field intensity **H** which is measured inside the object by special pulse sequences in an MRI system. A significant problem arises at this point in that curl operation requires all three components of **H** to be measured. Normally, only longitudinal component of **H,** namely $\mathbf{H}_z$, can be obtained by a single MRI experiment. Measurement of all three components of **H** therefore necessitates the rotation of the object in the MRI system. This is a highly impractical situation and motivates us to find new algorithms to reconstruct resistivity images by using only one component of **H**. The resistivity reconstruction problem of MR-EIT can be formulated as a system of first order hyperbolic partial differential equations, where log-resistivity is the dependent variable. Our proposed algorithm requires the Laplacian of the measured $\mathbf{H}_z$ and a forward solver to estimate **J** from any given resistivity distribution for a given current injection profile. From numerical simulations we find that the iterative application of the algorithm converges to a log-resistivity distribution where $\left\|\mathbf{H}_z^m - \mathbf{H}_z^c\right\|$ is used as the error criterion ($\mathbf{H}_z^m$ and $\mathbf{H}_z^c$ are the measured and calculated magnetic field intensities respectively). It is necessary to apply at least two current injection profiles such that internal current densities at each point of the object are non-aligned. 2D and 3D simulations are performed to investigate the convergence properties of the proposed algorithm.

Local Scanning of a Medium by Electrical Impedance Endotomography

Jacques Jossinet and Anne Desseux

National Institute for Health and Medical Research INSERM U556, Lyon, France

The visualisation of small organs by Electrical Impedance Tomography (EIT) suffers from the unavoidable decrease of sensitivity and resolution at distance from electrodes, i.e. in the deeper regions of the body. Furthermore, in the case of the prostate, the morphology of this part of the human body prevents the regular spacing of surface electrodes. The design of a urethral impedance probe for the scanning of the prostate lead to consider a modality, that was termed Electrical Impedance Endotomography (EIE), where the electrodes are located inside the region of interest instead of encircling it. In this modality, the electrodes are regularly placed around an insulating core. This approach results in significant differences with respect to conventional EIT. The present study reviews the similarities and dissimilarities between EIT and EIE. The points studied include the analysis of the boundary conditions, the sensitivity distribution and the influence of the signal-noise ratio. The authors have proposed a 2-D model of EIT. This model gave rise to analytical equations for potential, electric field and current density. These equations were used in the calculation of the sensitivity matrix used for the investigation of the above features. The reconstruction of images from data sets collected in vitro using a 16-electrode probe confirms the findings of the theoretical study. The first results showed that EIE enables the scan a medium in a range extending to about 4 times the radius of the probe, under the described experimental conditions. Hardware improvement is presumably possible. The major advantage with respect to EIT is the known geometry of the boundary surface containing the electrodes. The method is potentially applicable to other parts of the body, provided there is an invasive or a natural way to pass a probe.

Adaptation of EIT reconstruction algorithms to electrical impedance endotomography

Anne Desseux and Jacques Jossinet

as above

Electrical Impedance Endotomography (EIE) is a modality of Electrical Impedance Tomography (EIT) where the electrodes are located in the middle of the region of interest (ROI) instead of at its periphery. This modality enables the imaging of deep and small organs of the human body that EIT cannot visualize in good conditions. One major difference with EIT is that no physical boundary limits the region sensed by an EIE. In practice, the contributions of distant points do not significantly differ from noise, so that the actual sensitivity domain is finite. In EIE, the known geometry of the boundary enables distortion-free image reconstruction. The governing equation is the same in both modalities. One may therefore presume that the algorithms used in EIT image reconstruction are usable in EIE. The purpose of the present study was the adaptation of two EIT image reconstruction algorithms and the assessment of the influence of mesh parameters on the quality of reconstructed image. A too small reconstruction domain would exclude points of significant sensitivity. A too large mesh would include pixels of too small sensitivity, leading to increased ill conditioning of the sensitivity matrix. The tested algorithms were the NOSER algorithm and filtered back projection algorithm. A prototype 16-electrode probe and a single frequency system enabled in vitro data collection. The calculation of the sensitivity matrix involved the analytical 2-D model formerly developed for EIE. The results showed that the parameters of the mesh (mesh dimension and pixel size) have strong influence on image reconstruction. The conclusion is that NOSER and back-projection algorithms are usable in EIE with appropriate mesh definition.

Electrical impedance measurements in inferior limbs of the pregnants. preliminary results.

M. Korotkova†, A. Karpov†, V. Cherepenin‡, A. Korjenevsky‡

†Clinical Hospital # 9, Yaroslavl, Russia
‡Institute of Radio-Engineering and Electronics of Russian Academy of Sciences, Russia

In available printed materials we could not find any information on the use of electrical impedance tomography for studying arterial, venous and tissue blood flow in inferior limbs of the pregnant. We measured electrical impedance changes in inferior limbs of healthy pregnant women in different periods of pregnancy (6-21 weeks). We examined 14 women. We used 16-electrode single -frequency (8kHz, 0.5 mA) single- channel electrical impedance tomograph for obtaining static images which had been developed in the Institute of Radio-Engineering and Electronics, Russian Academy of Science. Computerized scanning of inferior limbs was made in the upper third of the left and right shin when the pregnant was in the left lateral and standing positions. For the measurements we used steel round electrodes (6 mm in diameter) fixed around a pregnant shin with the help of a rubber belt on its upper third. We showed similarity and repeatability of images at repeated measurements from the same pregnant woman under various conditions. We qualitatively evaluated images of the shin in electrical impedance tomograms: anatomic accuracy, anatomic topographic correlation. While interpreting the digital data it was found out that electrical conductivity in the norm (v, conventional units) in vascular and extravascular zones between the right and left shins truly differs only in thee left lateral position (left shin - V lateral = 1.116; std lateral =0.44; right shin - V lateral = 1.605; std lateral =0.665; p¡0.05). In a standing position re- liability of differences disappears (p¿0.05). While comparing electrical conductivity in vascular and extravascular zones of the same shin in lateral and standing positions in the norm no reliable differences were obtained (left shin - V lateral = 1.116; std lateral =0.44; right shin - V standing = 1.544; std standing =1.19; p¿0.05, right shin – V lateral = 1.605; std lateral =0.665; V standing = 1.726; std standing =0.818; p¿0.05). While comparing electrical conductivity between vascular and extravascular zones of the same shin in the norm reliability of differences was seen only in the lateral position. The paper is illustrated with electrical impedance tomograms and tables.

Fast calculation of the sensitivity matrix in magnetic induction tomography by tetrahedral edge finite elements

K. Hollaus†, C. Magele†, R. Merwa‡, H. Scharfetter‡

†Institute for Fundamentals and Theory in Electrical Engineering, IGTE, Technical University Graz, 8010 Graz, Austria
‡Institute for Biomedical Engineering, Technical University Graz, 8010 Graz, Austria

Introduction: The sensitivity analysis and the solution of the inverse problem of magnetic induction tomography (MIT) require the calculation of the Jacobian matrix of the measured data with respect to the conductivity. The use of finite differences is extremely cumbersome because of the high computational costs of the related eddy current problem (ECP). To facilitate the calculation the finite element method (FEM) is used exploiting a published sensitivity theorem (ST). Method: The method is based on the application of the reciprocity theorem to an ECP. Eddy currents are generated by a time harmonic magnetic field in a conducting region by an excitation coil. A sensor coil observes the resulting magnetic field. The ST represents a relation between the change of induced voltage (IV) in a sensor coil due to small perturbation in the complex conductivity and magnetic permeability. The ECP to be simulated is formulated in terms of a modified electric scalar potential represented by nodal finite elements in the conducting region and of a reduced magnetic vector potential valid in the entire problem region approximated by tetrahedral edge finite elements (FE). The numerical implementation of the ST by the FEM yields the sensitivity matrix (SM). The SM has to be multiplied only by a vector whose entries are the small perturbations of the material assigned to the FEs to get the change of the IV. Results: To validate the method a small but representative ECP has been studied. Results obtained by this method have been compared with those obtained by finite changes of the conductivity in the perturbed region. A satisfactory agreement has been observed. Discussion: The computation of the SM requires the solutions of separate ECPs, one for each coil. Once the SM is known simple arithmetic operations (AOs), i.e., a multiplication of a matrix by a vector, have to be carried out to get the change of the IV. The computational costs of the AOs are negligible small compared to the simulation of the basic ECPs.

Geometric Multigrid to accelerate the solution of quasi-static field problems by tetrahedral finite elements

K. Hollaus†, C. Magele, B. Weiß1, H. Hutten‡

†Institute for Fundamentals and Theory in Electrical Engineering, IGTE, Graz University of Technology, 8010 Graz, Austria
‡Institute for Biomedical Engineering, Graz University of Technology, 8010 Graz, Austria

Introduction: In electrical impedance tomography (EIT) an inverse problem has to be solved, where a quasi-static field problem (QSFP) represents the forward problem. To accelerate the solution of QSFP by the finite element method (FEM) geometric multigrid (GM) is exploited. Method: The FEM is applied to simulate the QSFP resulting in large linear equation systems (LLESs), which have to be solved efficiently approximated by iterative methods. The Fourier analysis of the arising residuum shows that the high frequent components with respect to the finite element (FE) grid size vanish already after few iterations. However, relatively many iterations are required to minimize the low frequent components. This fact has led to the idea to operate with different coarser grids to eliminate the low frequent parts efficiently, too. The coarse grid is used to pick up the geometry of biomedical applications, i.e. the different compartments defined by the varying material properties. The fine grid serves for an accurate solution of the field problem. One finite element of the coarse grid is subdivided into eight small ones leading to the so called nested multigrid. After few iterations on the fine grid the residuum is determined and transferred to the coarse grid facilitating a fast computation of a correction to the rough solution on the fine grid. In the next step the correction is added to the previous solution on the fine grid. Then further iterations are carried out on the fine grid and so on. To take advantage of GM optimally the two-grid algorithm described above is extended to several grids for practical applications. Results: To examine the GM technique small but representative QSFPs have been investigated. Results obtained by GM have been compared with solutions obtained by using the fine grid only. It turned out that GM is essentially faster than using the fine grid only. Discussion: The additional effort to generate the grids and the associated memory requirements can be justified by the essentially faster solution

Joining AC-electrokinetic techniques: Increasing the resolution for cellular structures and molecular properties

Jan Gimsa

University of Rostock, Department of Biological, Chair of Biophysics, Gertrudenstr. 11A, D-18057 Rostock, Germany. Tel: 0049 381 2037, fax: 0049 381 2039, e-mail: jan.gimsa@biologie.uni-rostock.de

Dielectric spectroscopy when based on AC-electrokinetic effects investigates the frequency dependence of orientation (electro-orientation, EO), deformation, translation (dielectrophoresis, DP), rotation (electrorotation, ER) or aggregation of single cells or particles [1]. The observed forces arise from the interaction of induced charges with the inducing field and can also be exploited for handling or manipulating microscopic and submicroscopic particles like cells, organelles, supramolecular structures, viruses or artificial colloids. The high resolution of the techniques for the electric object parameters allows to resolve new polarization effects and to follow time-dependent parameter changes at the single particle or cell level. When methods like DP, ER and EO are applied to one object each method provides particular frequency spectra. Of course, the spectra are not independent of one another since each spectrum reflects the dielectric properties of the same object. In principle, all spectra can be predicted if the dielectric properties of the object are known. Unfortunately, this situation is unrealistic for biological cells. In experiments on chicken red blood cells, it was found that model parameters which satisfactorily described both, the DP and ER spectra, could predict the EO behavior albeit with large deviations. It is assumed that the resolution of electric properties of the compartments of a cell model with a given subcellular geometry will be the higher the more methods are employed. Thus, the combination of methods will contribute to better parameter sets. The higher resolution will contribute to the exploration of the cytoplasmic and membrane dielectric properties depending on electric surface, interfacial, bulk and molecular properties in an in vivo environment. This will not only be of importance in particle technologies but also lead to a better understanding of the subcellular mechanisms of energy absorption ("electro-smog").

References

[1] J. Gimsa, 2001. Characterization of particles and biological cells by AC-electrokinetics. in: A.V. Delgado (ed.) Interfacial Electrokinetics and Electrophoresis. Marcel Dekker Inc., New York. pp. 369-400

Low frequency electrical bioimpedance for the detection of inflammation and dysplasia in Barrett's oesophagus

CA Gonzalez-Correa †,#, BH Brown †,RH Smallwood †, TJ Stephenson ‡, CJ Stoddard ‡, KD Bardhan §

†Department of Medical Physics and Clinical Engineering, University of Sheffield, Sheffield, UK.
‡Royal Hallamshire Hospital, Sheffield, UK.
§Rotherham District General Hospital, Rotherham Hospitals NHS Trust Rotherham, UK.
#Departamento de Fsica, Universidad de Caldas, Manizales, Colombia, South America.

Keywords: Barrett's Oesophagus, Bio-electrical Impedance, Squamous Epithelium, Columnar Epithelium, Inflammation, Dysplasia, Adenocarcinoma.

We have been investigating the electrical changes accompanying structural changes from normal squamous tissue to adenocarcinoma in Barrett's Oesophagus. We illustrate this pathway in the figure below. 258 biopsies were analysed from resected tissue taken from 32 patients. We correlate the electrical resistivity (R) at 9.6 kHz and their histopathological interpretation. Inflammation seems to operate in two different ways depending on the tissue type. In squamous it produces an increase in resistivity, perhaps due to the formation of tight junctions, which are not seen in normal oesophageal tissue. In columnar tissue, the results suggest a small but statistically significant decrease of electrical impedance with inflammation (from R = 4.9 Ohm m to R = 4.2 Ohm m, p = 0.016) and a larger decrease when dysplasia is present (R = 3.4 Ohm m, p = 0.040). Low frequency electric current flows through the extra-cellular space and either its widening or the disruption of the tight junctions (or both) will decrease the resistance. With adenocarcinoma, the resistivity at low frequency increases, probably due to the fact that, when compared to the columnar tissue, the cell density (vol/vol) increases, reducing the extra-cellular space. If this method is validated further, then it could be used to obtain guided biopsies from patients undergoing surveillance programs for Barrett's oesophagus. We aim to refine this technique using a new system which makes measurements at lower frequencies.

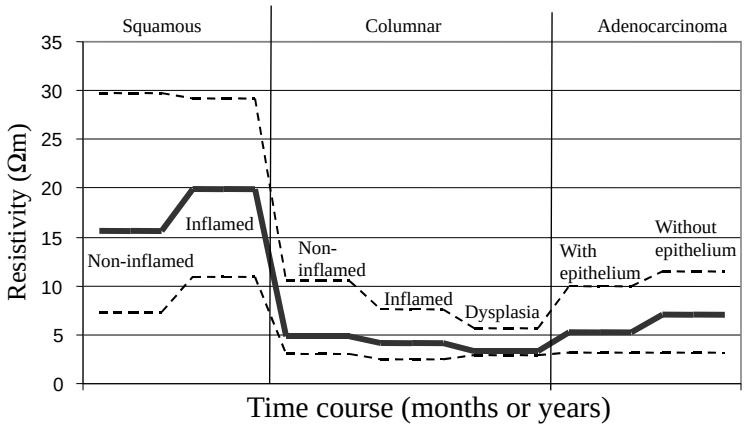

Figure 1: Expected sequence of changes in electric resistivity accompanying the sequence of tissue changes in Barrett's oesophagus. Values are the median (thick line in the middle) and the 90th (dashed line above) and 10th (dashed line below).